

Quantum diffraction grating with cold atoms in an optical lattice

Adhip Agarwala, Madhurima Nath, Jasleen Lugani, K. Thyagarajan and Sankalpa Ghosh

Department of Physics, Indian Institute of Technology Delhi, New Delhi-110016, India

(Dated: February 24, 2012)

Abstract

Light transmission or diffraction from different quantum phases of cold atoms in an optical lattice have recently come up as a useful tool to probe such cold atomic systems. The periodic nature of the optical lattice potential closely resembles the structure of a diffraction grating in real space, but loaded with a strongly correlated quantum many body state which interacts with the incident electromagnetic wave, a feature that controls the nature of the light transmission or dispersion through such quantum medium. The paper contains a detailed analysis of such a quantum diffraction grating. We have particularly studied how the dispersion shift induced by the cavity changes as a function of the relative angle between the cavity mode and the optical lattice.

PACS numbers: 03.75.Lm, 42.50.-p, 37.10.Jk

I. INTRODUCTION

Ultra cold atomic condensates loaded in an optical lattice [1, 2] provide a unique opportunity to study the properties of an ideal quantum many body system. After the first successful experiment in this field [3] where a quantum phase transition from a Mott Insulator(MI) to Superfluid(SF) phase was observed, extensive theoretical as well as experimental study in this direction took place. The field continues to be a frontier research area of atomic and molecular physics, quantum condensed matter systems as well as quantum optics simultaneously, and holds promise for application in fields like quantum metrology, quantum computation and quantum information processing [4, 5].

The relevance of the field of ultra cold atomic condensates to quantum optics was suggested much earlier when it was pointed out that the refractive index of a degenerate Bose gas gives a strong indication of quantum statistical effects [6] and the interaction between quantized modes of light and such ultra-cold atomic quantum many body system is going to lead to a new type of quantum optics [7]. Subsequently, it was pointed out that the optical transmission spectrum of a Fabry-Perot cavity loaded with ultra cold atomic BEC in an optical lattice can clearly distinguish between a SF and MI state [8] and may be used as an alternative way of detecting such phase transition without directly perturbing the cold atomic ensemble through absorption spectroscopy. A successful culmination of some of these theoretical predictions happened with the recent experimental success of realization of a strongly coupled atom-photon system where an ultra cold atomic system is placed inside an ultra-high finesse optical cavity[9, 10], such that a photon in a given quantum state can interact with a large collection of atoms in same quantum mechanical state and thereby enhancing the atom-photon coupling strength. As an aftermath, a host of interesting phenomena such as cavity optomechanics [11], observation of optical bistability and Kerr nonlinearity [12] has been experimentally achieved with such systems. It may be also mentioned in this context that Bragg diffraction pattern from a quasi-two dimensional Mott Insulator, but without any cavity, was also recently been observed experimentally [13].

The theoretical progress in understanding such atom-photon systems involving ultra cold atomic condensates is also impressive. A series of work by the Innsbruck group [8, 14–20] clearly pointed out how the optical properties of the cavity reveals the quantum statistics of these many body systems. In another set of work, cavity induced bistability in the MI

to SF transition either due to strong cavity-atom coupling [21] or due to the change in the boundary condition of the cavity [22] has been studied and its relation to cavity quantum optomechanics [23, 24] has also been explored. The self organization of atoms in a multimode cavity due to atom-photon interaction leading to the formation of exotic quantum phases and phase transition [25–27] is another major development in this direction. The recent observation of Dicke quantum phase transition through which a transition to a supersolid phase was achieved [28] through such self organization is an important experimental landmark in this direction.

The physics of ultracold atoms loaded inside an ultrahigh-finesse Fabry-Perrot cavity can be analyzed from two different, but highly correlated perspectives. For example, ultra cold atomic ensemble loaded in such optical lattices with short range interaction can exist in two different types of quantum phases, MI and SF. The former is a definite state in the Fock space with well defined number of particles at each lattice site and lacks phase coherence between the atomic wavefunctions at different sites. The latter is a superposition of various Fock space states and has phase coherence. A phase transition between these phases takes place as the lattice depth varies. The statistical distribution of atomic number that characterizes these many body states consequently influences the transmitted or diffracted electromagnetic wave through atom-light interaction and thereby changes the dielectric response of such cavity in the same way as the change of material leads to the change in refractive index.

From another perspective, the periodic optical lattice potential forms a grating like structure in the real space, but now each slit of the grating contains ultra cold atoms in their quantum many-body state, that interacts with the light quanta of the electromagnetic field through the dipole interaction. Such a system has been dubbed as a quantum-diffraction grating in the literature [8]. It is well known that any quantum mechanical scattering process leads to the diffraction effect and thus such effect is ubiquitous in various quantum systems. As early as in 1977 in a review article by Frahn [29] an overview of such wide range of quantum mechanical diffraction process was presented in a common theoretical framework by comparing them with classical optical diffraction. Though some element of such quantum diffraction is also present in atom-photon system under consideration, it is unique in the sense that here electromagnetic wave is getting diffracted by a quantum phase of matter wave loaded inside a cavity. A classical description of such diffraction of electromagnetic wave by a single atom or an atomic ensemble placed inside a cavity was also discussed in

detail in ref. [30].

It has been pointed out [31] that in ultra cold fermionic atoms, the diffraction properties of such quantum-diffraction grating is strongly dependent on the mode of quantization of the cavity. In the limit of very large cavity detuning also, the features of such quantum diffraction for ultra cold bosonic atoms and its departure from the classical behavior has been studied [14]. The result from these earlier studies indicate that a detailed analysis of the diffraction properties of such quantum diffraction grating has the potential to characterize the many-body quantum states of ultra cold atoms in more detail. Since the relevant experimental system is already available, such a study is even more encouraging. In the current paper we carry an analysis of the diffraction property of such quantum diffraction grating in detail.

The plan of the paper is as follows. In the next section we begin with a brief review of the formalism that is used to calculate the transmission from such a cavity loaded with ultra cold atoms in optical lattice. We shall particularly discuss the cases when a single mode and two modes are excited in the Fabry-Perot cavity and show how the transmitted intensity through the cavity will be calculated in these two cases. The particular emphasis in this work will be on how the transmitted intensity changes as one varies the relative angle between the optical lattice and pump laser(s) that excite the modes. Using this theoretical framework in the next sections we shall present our result which will show how the transmitted intensity varies both for the MI and SF phases under different conditions. An analysis of these results and their comparison against various classical diffraction pattern provides us a sound understanding of this quantum diffraction phenomena. Finally we extend the results to a ring shaped cavity and will show how cavity quantization procedure changes the transmitted intensity.

II. MODEL

The physical system we describe is depicted in Fig. 1 and consists of N identical two-level bosonic atoms placed in an optical lattice of M sites inside a Fabry-Perot cavity. K sites among these are illuminated by cavity modes, pumped into the system by external lasers. We shall consider both the cases, in which single cavity mode, and two cavity modes will be excited.

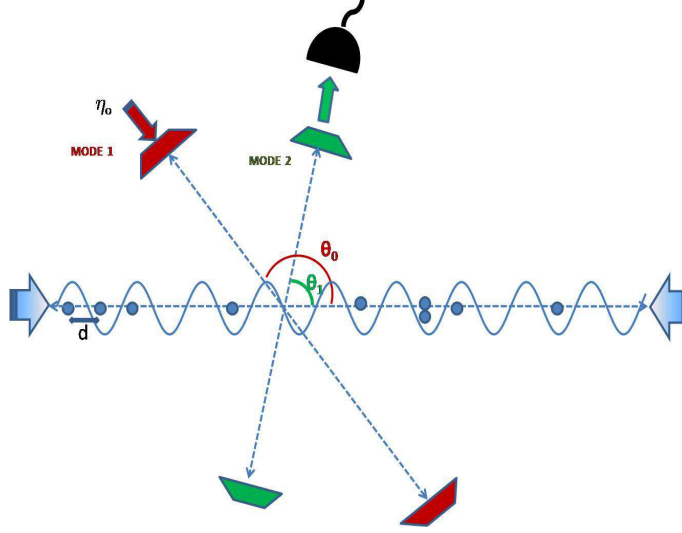


FIG. 1: (Color Online) Schematic diagram for cold atoms in an optical lattice loaded in a cavity. The optical lattice is created from two counter propagating laser beams and has a site spacing of length d . The two standing wave cavity modes, MODE 1 and MODE 2 are at angles θ_0 and θ_1 with the axis of the optical lattice respectively. The MODE 1 is being pumped by a pump laser with amplitude η_0 while MODE 2 is not being pumped and is used to collect the scattered photons by a detector. In the single mode case, the detector is also on MODE 1 and has not been shown in this figure.

These modes can be composed of either standing waves(SW) or travelling waves(TW). The setup given in Fig. 1 can realize standing waves; whereas later we shall discuss the corresponding setup for travelling wave solutions. Such a system was studied in [8, 14–20] and for a detailed treatment, the reader may refer to [14]. Here we describe this theoretical framework briefly.

The above mentioned system can be theoretically modeled as a collection of N two level atoms, that are approximated as linear dipoles, to account for their interaction with the quantized electric field of the cavity modes. To describe the system through an effective Hamiltonian one then uses well known rotating wave approximation in which all fast oscillating terms in the Hamiltonian are neglected. The excited state of the two level atoms is then adiabatically eliminated assuming that the cavity modes are largely off resonant to energy difference between the atomic levels. Thus in the resultant system all the atoms are

in their ground states. The effective Hamiltonian arrived in this way is given by

$$\begin{aligned}
H = & H_f + J_0^{cl} \hat{N} + J^{cl} \hat{B} + \hbar g^2 \sum_{l,m} \frac{\hat{a}_l^\dagger \hat{a}_m}{\Delta_{ma}} \left(\sum_{j=1}^K J_{j,j}^{lm} \hat{n}_j \right) \\
& + \hbar g^2 \sum_{l,m} \frac{\hat{a}_l^\dagger \hat{a}_m}{\Delta_{ma}} \left(\sum_{\langle j,k \rangle} J_{j,k}^{lm} \hat{b}_j^\dagger \hat{b}_k \right) + \frac{U}{2} \sum_{j=1}^M \hat{n}_j (\hat{n}_j - 1)
\end{aligned} \tag{1}$$

Here

$$H_f = \sum_l \hbar \omega_l \hat{a}_l^\dagger \hat{a}_l - i \hbar \sum_l (\eta_l^*(t) \hat{a}_l - \eta_l(t) \hat{a}_l^\dagger)$$

where first term denotes the free field Hamiltonian and the second depicts the interaction of classical pump field with cavity mode, \hat{a}_l is the annihilation operators of light modes with the frequencies ω_l , wave vectors \mathbf{k}_l , and mode functions $u_l(\mathbf{r})$. $\eta_l(t) = \eta_0 e^{-i\omega_p t}$ is the time dependent amplitude of the external pump laser of frequency ω_p that populates the cavity mode.

Here $J_{j,k}^{cl}$ correspond to the matrix element of the atomic Hamiltonian in the site localized Wannier basis, $w(\mathbf{r} - \mathbf{r}_j)$, namely

$$J_{j,k}^{cl} = \int d\mathbf{r} w(\mathbf{r} - \mathbf{r}_j) H_a w(\mathbf{r} - \mathbf{r}_k) \tag{2}$$

where $H_a = -\frac{\hbar^2 \nabla^2}{2m_a} + V_{cl}(\mathbf{r})$ is the Hamiltonian of a free atom of mass m_a in an optical lattice potential $V_{cl}(\mathbf{r})$. Therefore, $J_0^{cl} = J_{j,j}^{cl}$, and $J^{cl} = J_{j,j\pm 1}^{cl}$ are respectively the onsite energy and the hopping amplitude of proto-type Bose Hubbard model given in [1]. At the atomic site j , \hat{b}_j is the annihilation operator, and $\hat{n}_j = \hat{b}_j^\dagger \hat{b}_j$ is the corresponding atom number operator, $\hat{N} = \sum_{j=1}^M \hat{n}_j$ denotes the total atom number and $\hat{B} = \sum_{j=1}^M \hat{b}_j^\dagger \hat{b}_{j+1}$.

The coefficients $J_{j,k}^{lm}$ is similar to $J_{j,k}^{cl}$, but now generated from interaction between atoms and quantized cavity modes and is given by ,

$$J_{j,k}^{lm} = \int d\mathbf{r} w(\mathbf{r} - \mathbf{r}_j) u_l^*(\mathbf{r}) u_m(\mathbf{r}) w(\mathbf{r} - \mathbf{r}_k) \tag{3}$$

$\Delta_{la} = \omega_l - \omega_a$ denotes the cavity atom detunings where ω_a is the frequency corresponding to the energy level separation of the two-level atom and g is the atom-light coupling constant. Thus the fourth and fifth term in (1) respectively contribute to the onsite energy and hopping amplitude due to the interaction between atoms and quantized cavity modes.

In the last term, $U = \frac{4\pi a_s \hbar^2}{m_a} \int d\mathbf{r} |w(\mathbf{r})|^4$, where a_s denotes the s -wave scattering length and gives the onsite interaction energy. For a sufficiently deep optical lattice potential $V_{cl}(\mathbf{r})$, the overlap between Wannier functions can be neglected. In this limit $J^{cl} = 0$ and $J_{j,k}^{lm} = 0$ for $j \neq k$. Such Wannier functions can be well approximated as delta functions centered at lattice sites \mathbf{r}_j and consequently $J_{j,j}^{lm} = u_l^*(\mathbf{r}_j)u_m(\mathbf{r}_j)$.

The above Hamiltonian in (1) describes the zero temperature quantum phase diagram of ultra cold bosonic atoms loaded in an optical lattice placed inside a optical cavity. This is because their many body quantum mechanical ground state can exist in various quantum phases [1, 3] as a function of parameters like U and J . In the subsequent analysis in this work, the physical system that diffracts the photons is therefore a novel type of quantum diffraction grating not only because the diffracting medium corresponds to a quantum phase of ultra cold atoms, but also due to the fact that it is embedded in a optical lattice/grating like structure in real space which in turn affects the nature of such quantum phase. As we shall point out, one particular way of understanding the nature of such quantum diffraction and differentiate from classical diffraction or any other quantum diffraction [29] is to study it as a function of the relative angle between the cavity mode and direction of the optical lattice in which the cold atoms are loaded. Quantum diffraction of electromagnetic wave by such ultra cold atomic condensate inside an Fabry-Perot cavity, but without loading them in an optical lattice (other than the one dynamically generated due to cavity-atom coupling), was already experimentally studied in ref [11] in the context of cavity quantum optomechanics. Thus the physical system under consideration is very much realizable experimentally. We start our discussion by briefly outlining the relevant theoretical framework to understand such quantum diffraction following ref [14].

III. METHODOLOGY

From the atom-photon Hamiltonian (1), the Heisenberg equation of motion of the photon annihilation operator \hat{a}_l is given by

$$\dot{\hat{a}}_l = -i\omega_l \hat{a}_l - i\delta_l \hat{D}_{ll} \hat{a}_l - i\delta_m \hat{D}_{lm} \hat{a}_m - \kappa \hat{a}_l + \eta_l(t) \quad (4)$$

with $\hat{D}_{lm} \equiv \sum_{j=1}^K u_l^*(\mathbf{r}_j)u_m(\mathbf{r}_j)\hat{n}_j$, where $l \neq m$ and $\delta_l = g^2/\Delta_{la}$. κ is the cavity relaxation rate introduced phenomenologically. The first, fourth and the fifth terms on the right hand side

correspond to property of light transmission through an empty cavity. The second and third terms give the information about the atom-light interaction in the cold atomic condensates.

A. Single Mode

First we shall consider the case when a single cavity mode is excited. From the stationary solution for one mode case, namely $\dot{\hat{a}}_l = 0$ we obtain the expression for the corresponding photon number operator as,

$$\hat{a}_0^\dagger \hat{a}_0 = \frac{|\eta_0|^2}{(\Delta_p - \delta_0 \hat{D}_{00})^2 + \kappa^2} \quad (5)$$

Here $\Delta_p = \omega_{0p} - \omega_0$ is the probe-cavity detuning and $\hat{a}_l = \hat{a}_0$. In this case $\hat{a}_m = 0$ and $\hat{D}_{l,m} = \hat{D}_{00}$. The single mode transmission through the cavity is calculated by taking the expectation value of the above expression in given many-body atomic ground state. As expected such an expression is similar to the standard Breit Wigner form. However \hat{D}_{00} is in terms of the Fock space operators acting on the atomic ensemble, revealing the statistical properties of the quantum matter of ultra cold atoms.

Now in the denominator of the above expression the shift in frequency is determined by the eigenvalue of the operator \hat{D}_{00} , which is dependent on both the atomic configuration, *i.e.*, the number of illuminated atoms and the mode functions. For plane standing waves the mode function, $u(\mathbf{r}_j)_{SW} = \cos(\mathbf{k} \cdot \mathbf{r}_j + \phi)$ where ϕ is constant phase factor which has been set to zero and \mathbf{r}_j denotes the position vector of the j th site on the optical lattice. Here we consider a one dimensional optical lattice with site spacing d . For a cavity mode of wavelength λ incident at an angle θ with the optical lattice, $u(\mathbf{r}_j)_{SW} = \cos(\frac{2\pi}{\lambda} j d \cos \theta)$. We assume the cavity mode wavelength to be $2d$ and thus, the mode function is $u(\mathbf{r}_j)_{SW} = \cos(j\pi \cos \theta)$, where $j \in I$. For such standing waves, the factor \hat{D}_{00} becomes,

$$\hat{D}_{00} = \sum_j u_l^* u_l \hat{n}_j = \sum_{j=1:K} \cos^2(j\pi \cos \theta) \hat{n}_j \quad (6)$$

where K are the number of illuminated sites. This shows that shift in the cavity resonant frequency is dependent on the relative angle of the cavity mode with the optical lattice. To simplify the analysis, here it has been assumed that while changing this angle, the light beam waist is modified in a way that we always illuminate only fixed K sites. However, as

explained below, a few sites fall at intensity minima of the cavity mode, thus changing the effective number of illuminated sites.

For example in Fig. 2a we show the cases when light with wavelength($=2d$) is incident at $\theta = 0^\circ$ and $\theta = 60^\circ$. When the angle $\theta = 0^\circ$, all the atoms are at the points of maximum intensity or the anti-nodes of the cavity mode wavelength. Thus all the atoms are illuminated. When θ changes to 60° , the projected wavelength along the optical lattice direction changes and a few atoms which were at the maxima points are now placed at the points of minimum(or zero) intensity or nodes. Thus now only the alternate sites are illuminated as can be seen in Fig. 2a. Therefore, the effective number of illuminated sites in the lattice at $\theta = 60^\circ$ reduces to half its value at $\theta = 0^\circ$. Hence the dispersive shift varies with the change in the relative angle of the cavity mode and the optical lattice.

1. Mott Insulator

We shall first consider the case when the ground state of the atomic ensemble is a MI, ie., a single state in the Fock space.

$$|\Psi\rangle = |n, n, n, \dots, n\rangle \quad (7)$$

with $n = \frac{N}{M}$. This state is also an eigenstate of the operator \hat{D}_{00} with eigenvalue $F(\theta, K)n$ where

$$F(\theta, K) = \frac{1}{2} \left[K + \frac{\sin(K\pi\cos\theta)}{\sin(\pi\cos\theta)} \cos((K+1)\pi\cos\theta) \right] \quad (8)$$

which has been calculated using (6). The corresponding transmission spectrum will be proportional to the photon number, which is given by

$$\langle \Psi | \hat{a}_0^\dagger \hat{a}_0 | \Psi \rangle = \frac{|\eta_0|^2}{(\Delta_p - \delta_0 F(\theta, K)n)^2 + \kappa^2} \quad (9)$$

This has been plotted in Fig.2b with the angle θ and detuning Δ_p/δ_0 .

Let us first point out that from the left and the right side, the intensity plot is strikingly similar to the real space intensity variation in classical light wave diffraction from a straight edge [32, 33] even though intensity variation in these two cases are function of completely different set of physical variables. We shall here briefly explain this apparent similarity inspite of these differences. Here we have plotted the variation of the photon number as a function of the angle θ and the cavity detuning. Therefore the plot is not an intensity

plot in the real space. At each value of θ , we obtain a maximum intensity at that value of the dispersion shift which corresponds to the number of atoms illuminated in the lattice at that angle. As the number of illuminated atoms changes with the change in the relative angle θ so the dispersive shift takes different values depending on the atomic arrangement. Nevertheless, the similarity stems from the fact that the factor \hat{D}_{00} which is written in the following form,

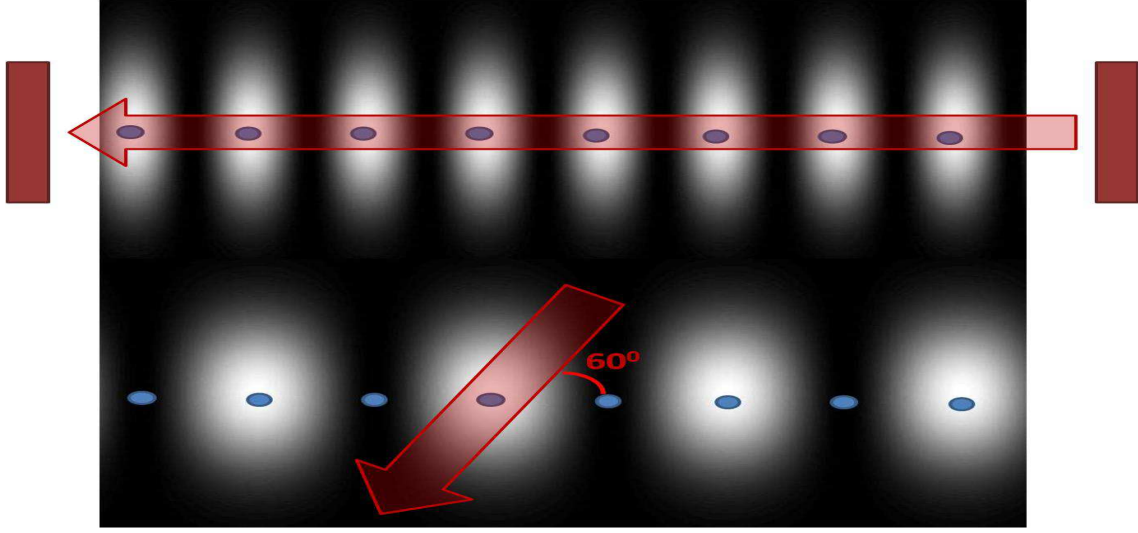
$$\hat{D}_{00} = \sum_{j=1:K} \frac{1}{2} [1 + \cos(4\pi j \cos^2 \frac{\theta}{2})] \hat{n}_j \quad (10)$$

mathematically has a similar form of the Fresnel integral, encountered in the intensity profile for a straight edge diffraction pattern. There the intensity is a function of $C(\tau)$ given by

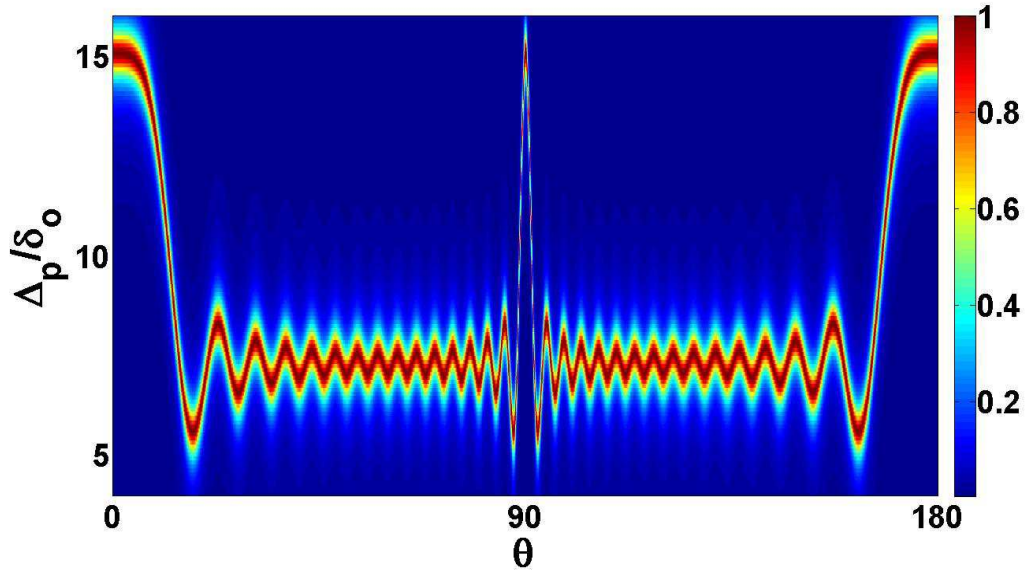
$$C(\tau) = \int_0^\tau \cos(\pi x^2/2) dx \quad (11)$$

where τ is dependent on the geometry of the system including the distance from screen. An increase in τ implies, the evaluation of intensity at a point farther from the straight edge. The oscillating behavior of the intensity can be attributed to the functional dependence of Eq.(11). However, it is to be noted, that Eq.(10) involves a summation over the illuminated sites K , which is constant and the variation is plotted with respect to θ , which is the angle made by the cavity mode with lattice. This summation can be understood in the context of the lattice being discrete. But for a fixed K , as we change θ , we are effectively changing the number of illuminated sites, as mentioned earlier, and hence the nature of the plot seems similar.

Since the dispersion shift is an indicator of the refractive index of the medium, the above result suggests that the refractive index of a given quantum phase is dependent not only on the site distribution of the atomic number, but also on the angle between the propagation direction and the optical lattice. This is a unique feature of this system. It may be recalled that in well known optical phenomenon like Raman Nath scattering due to diffraction through a medium with periodically modulated refractive index [34] or in Brillouin scattering in non-linear medium [35], there is also a frequency shift due to dispersion of the transmitted electromagnetic wave through the medium. However the mechanism of the dispersion shift as a function of angle between the cavity mode and optical lattice as explained in the preceding discussion is fundamentally different from these cases.



(a)



(b)

FIG. 2: (Color Online) (a) The top part of this schematic shows the way atoms are present at the intensity maxima regions of the illuminating cavity mode when the optical lattice is illuminated at 0° . However, changing the angle by 60° results in the decrease of the number of illuminated sites to half. (b) Variation of the photon number (9) (color axis) with detuning $\frac{\Delta p}{\delta_0}$ and θ (in degrees) for $N=M=30$, $K=15$, $\kappa = 0.5\delta_0$, when the atoms are in a MI state and are illuminated by a single standing wave cavity mode.

2. Superfluid

Next we consider the case when the atoms are in SF phase. The SF wave function in the Fock space basis can be written as superposition state, namely

$$|\psi\rangle = \frac{1}{M^{N/2}} \sum_{\langle n_j \rangle} \sqrt{\frac{N!}{n_1!n_2!\dots n_M!}} |n_1, n_2, \dots, n_M\rangle \quad (12)$$

where n_j denotes the number of atoms at the j th site while $\langle n_j \rangle$ denotes a set of n_j for a particular Fock state. Unlike the MI case, here \hat{D}_{00} acts on a superposition of Fock states each of which is an eigenstate of this operator. Each such Fock state carries a different set of $|n_1, n_2, \dots, n_M\rangle$. Hence,

$$\langle \Psi | \hat{a}_0^\dagger \hat{a}_0 | \Psi \rangle = \frac{1}{M^N} \sum_{\langle n_j \rangle} \frac{N!}{n_1!n_2!\dots n_M!} \frac{|\eta_0|^2}{(\Delta_p - \delta_0 F_s(\theta, K, n_j))^2 + \kappa^2} \quad (13)$$

where, $F_s(\theta, K, n_j)$ is the eigenvalue of the operator \hat{D}_{00} acting on a particular Fock state. Here the F_s functions are generalization of the F function described in (8), for the case of SF phase in which the number of particles in each site is different as,

$$F_s(\theta, K, n_j) = \sum_{j=1:K} \cos^2(j\pi \cos\theta) n_j \quad (14)$$

where j is the site index and n_j is the occupancy of site j . It can be easily checked for $n_j = n$ for all j , $F_s = nF$.

The decomposition of the many body states in Fock space basis is now mapped in the frequency shifts of the cavity mode. The probabilistic weight factor is mapped in the intensity of the peak at that particular value of dispersion shift. At a particular angle of incidence, the singular peak of MI now breaks into multiple peaks with varied peak strengths and dispersion shifts. Each particular peak corresponds to a particular group of Fock states which have the same value of $F_s(\theta, K, n_j)$ as defined in Eq.(14). Now as the angle θ is being changed, the effective number of illuminated sites change. This changes the value of $F_s(\theta, K, n_j)$ as well as the set of Fock states which yield the same value of $F_s(\theta, K, n_j)$.

This can be understood clearly by taking a case where the number of Fock states involved is small. The corresponding states is few body correlated state which is a few body analogue of a superfluid state, where the number of Fock states involved is thermodynamically large. Consider the case when 2 atoms are placed in 3 sites among which the first 2 sites are

illuminated through a cavity mode. Here the average occupancy per site \bar{n}_j is $2/3$. At $\theta = 0^\circ$, $F_s(\theta, K, n_j) = \sum_{j=1}^K n_j$. Hence states yielding the same amount of shift would be $|2, 0, 0\rangle$, $|0, 2, 0\rangle$ and $|1, 1, 0\rangle$ and the corresponding value of $F_s(\theta, K, n_j)$ is $2\bar{n}_j$. On the other hand the states in which only a single atom is present in the illuminated sites, such as $|1, 0, 1\rangle$ or $|0, 1, 1\rangle$ will show a shift of just \bar{n}_j in the cavity frequency. However, $|0, 0, 2\rangle$ does not show any shift. Hence, the Fock states get distributed into groups having 3, 2, 1 states respectively, each group having a different value of the dispersion shift.

Now as the angle between the cavity mode and lattice is varied, the effective number of illuminated sites change and so changes the set of Fock states that has same $F_s(\theta, K, n_j)$. For example, at an angle 60° , only the alternate sites are effectively illuminated. Therefore in this case it is just the central site which is illuminated. Now under these circumstances, state $|0, 2, 0\rangle$ show a distinctively separate shift from the states $|2, 0, 0\rangle$ and $|1, 1, 0\rangle$. It may be recalled that at $\theta = 0^\circ$ all these states had the same shift. Moreover, now the states $|0, 1, 1\rangle$ and $|1, 1, 0\rangle$ will have same shift since only one atom gets illuminated in this case. Thus this evolution of Fock states is imprinted in the shift of the cavity frequency. This is shown in Fig.3a. The transmitted intensity from the cavity mode will be proportional to the photon number in that cavity mode. The color plot depicts this photon number whereas the black lines (explained in the legend of Fig.3a) correspond to the $F_s(\theta, K, n_j)\delta_0$ for each Fock state as a function of θ . As can be inferred wherever there is a maximum overlap of $F_s(\theta, K, n_j)$, the same location corresponds to the intensity peak. However an increase in the cavity decay rate κ shows that the individual peaks cannot be resolved as shown in Fig.3b.

B. Double mode

We shall now consider the case where two cavity modes are excited. The corresponding photonic annihilation operators are given by \hat{a}_0 and \hat{a}_1 . Following [8] we also assume that the probe is injected only into \hat{a}_0 , and hence, $\eta_1 = 0$. Also both have the same frequencies, *i.e.*, $\omega_0 = \omega_1$ and are oriented at angles θ_0 and θ_1 with respect to the optical lattice. From Eq.(4), $\dot{\hat{a}}_1 = 0$ yields

$$\hat{a}_1 = \frac{i\eta_0\delta_1\hat{D}_{10}e^{-i\Delta_p t}}{([\Delta_p - (\hat{\omega}_m + \hat{\Omega}_m)] + i\kappa)([\Delta_p - (\hat{\omega}_m - \hat{\Omega}_m)] + i\kappa)} \quad (15)$$

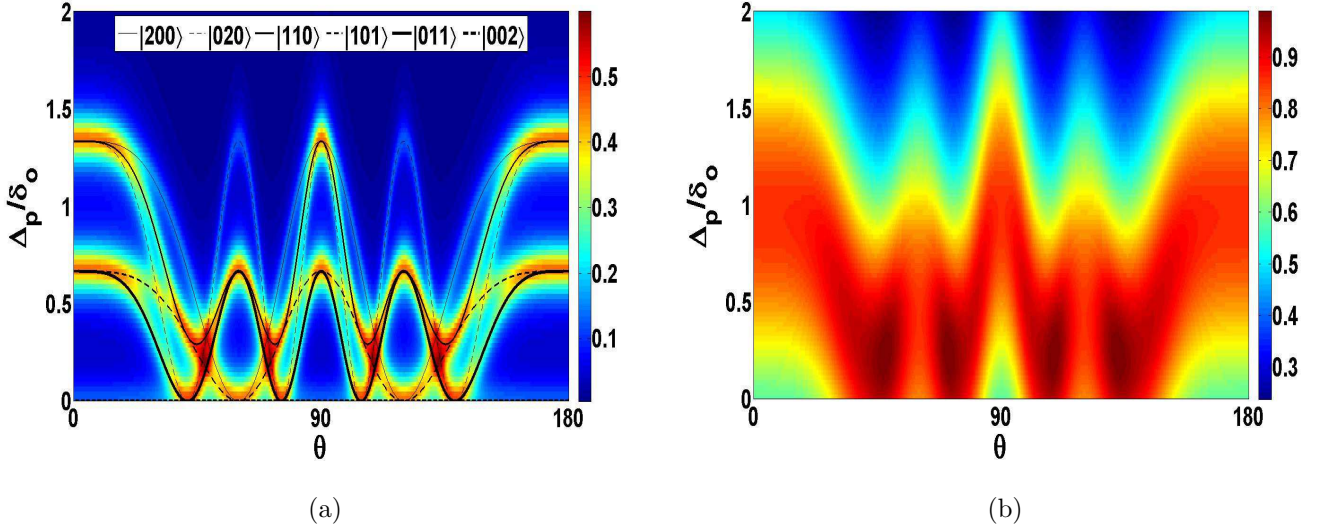


FIG. 3: (Color Online) Variation of the photon number (13) (color axis) with detuning $\frac{\Delta_p}{\delta_0}$ and θ (in degrees) for $N=K=2$, $M=3$, $\kappa=0.5\delta_0$ when the atoms are in SF state and are illuminated by a single standing wave cavity mode. In (a) with individual Fock states, represented by the black lines for $\kappa=0.1\delta_0$. In (b) for $\kappa=\delta_0$, the spectrum is blurred.

where

$$\begin{aligned}\hat{\omega}_m &= \frac{\delta_1}{2}(\hat{D}_{11} + \hat{D}_{00}) \\ \hat{\Omega}_m &= \sqrt{\frac{\delta_1^2(\hat{D}_{11} - \hat{D}_{00})^2}{4} + \delta_1^2 \hat{D}_{10}^\dagger \hat{D}_{10}}\end{aligned}\quad (16)$$

are now operators acting on the Fock space. This leads to

$$\hat{a}_1^\dagger \hat{a}_1 = \frac{\delta_1^2 \hat{D}_{10}^\dagger \hat{D}_{10} |\eta_0|^2}{([\Delta_p - (\hat{\omega}_m + \hat{\Omega}_m)]^2 + \kappa^2)([\Delta_p - (\hat{\omega}_m - \hat{\Omega}_m)]^2 + \kappa^2)} \quad (17)$$

Here, $\hat{D}_{01} = \hat{D}_{10}^\dagger$ and the expectation value of $\hat{a}_1^\dagger \hat{a}_1$ gives the photon number in this mode.

The above problem is equivalent to two linearized coupled harmonic oscillators which show mode splitting[8]. Briefly two such harmonic oscillators with natural frequencies ω_1 and ω_2 coupled to each other by a perturbation ζ , is described by the following set of coupled equations.

$$\begin{aligned}\frac{dx_1}{dt} &= -i\omega_1 x_1 + \zeta x_2 \\ \frac{dx_2}{dt} &= -i\omega_2 x_2 + \zeta x_1\end{aligned}$$

The normal modes of such a system are

$$\omega = \frac{\omega_1 + \omega_2}{2} \pm \sqrt{\left(\frac{\omega_1 - \omega_2}{2}\right)^2 + \zeta^2} \quad (18)$$

In the current problem, the shifted frequencies are given by the eigenvalues of

$$\hat{\omega}_m \pm \hat{\Omega}_m \quad (19)$$

acting on a particular state of the system. A particular case of interest will be when $\theta_0 = \theta_1$, this implies $\hat{D}_{00} = \hat{D}_{11} = \hat{D}_{10} = \hat{D}$. Then the photon number $\hat{a}_1^\dagger \hat{a}_1$ is

$$\hat{a}_1^\dagger \hat{a}_1 = \frac{\delta_1^2 \hat{D}^\dagger \hat{D} |\eta_0|^2}{[(\Delta_p - 2\hat{\Omega}_m)^2 + \kappa^2][\Delta_p^2 + \kappa^2]} \quad (20)$$

Thus one of the normal mode is independent of the atomic dispersion, however the other mode disperses by twice the value for a single mode. We shall now consider the case when the cavity modes are Standing Waves. The many body ground state shall be considered as either a MI or SF phase.

1. Mott Insulator

Again we shall first calculate the two mode transmission spectrum when the cavity contains atomic ensemble in a MI state given in (7). The operators \hat{D}_{00} and \hat{D}_{11} are given by (6) with eigenvalues $F(\theta_0, K)n$ and $F(\theta_1, K)n$. Also for such a MI state the operator \hat{D}_{10} is given by

$$\sum_{j=1:K} \cos(j\pi \cos\theta_0) \cos(j\pi \cos\theta_1) \hat{n}_j \quad (21)$$

When this operator \hat{D}_{10} acts on (7) its eigenvalue is given by $F(\theta_0, \theta_1, K)n$, where

$$F(\theta_0, \theta_1, K) = \frac{1}{2} \left[\left(\frac{\sin(K\pi \frac{\cos\theta_0 + \cos\theta_1}{2})}{\sin(\pi \frac{\cos\theta_0 + \cos\theta_1}{2})} \cos((K+1)\pi \frac{\cos\theta_0 + \cos\theta_1}{2}) \right) + \left(\frac{\sin(K\pi \frac{\cos\theta_0 - \cos\theta_1}{2})}{\sin(\pi \frac{\cos\theta_0 - \cos\theta_1}{2})} \cos((K+1)\pi \frac{\cos\theta_0 - \cos\theta_1}{2}) \right) \right]$$

The photon number is hence given by

$$\langle \Psi_{MI} | \hat{a}_1^\dagger \hat{a}_1 | \Psi_{MI} \rangle = \frac{\delta_1^2 |\eta_0|^2 [F(\theta_0, \theta_1, K)n]^2}{([\Delta_p - (f + \mathcal{F})]^2 + \kappa^2)([\Delta_p - (f - \mathcal{F})]^2 + \kappa^2)} \quad (22)$$

where,

$$f = \langle \Psi_{MI} | \omega_m | \Psi_{MI} \rangle = \frac{\delta_1}{2} (F(\theta_0, K) + F(\theta_1, K))n \quad (23)$$

$$\mathcal{F} = \langle \Psi_{MI} | \Omega_m | \Psi_{MI} \rangle = n \sqrt{\frac{\delta_1^2 (F(\theta_1, K) - F(\theta_0, K))^2}{4} + \delta_1^2 [F(\theta_0, \theta_1, K)]^2} \quad (24)$$

are the eigenvalues of the operators $\hat{\omega}$ and $\hat{\Omega}$ acting on MI state respectively. The normal modes are hence given by $f \pm \mathcal{F}$, and therefore the amount of mode splitting is given by $2\mathcal{F}$.

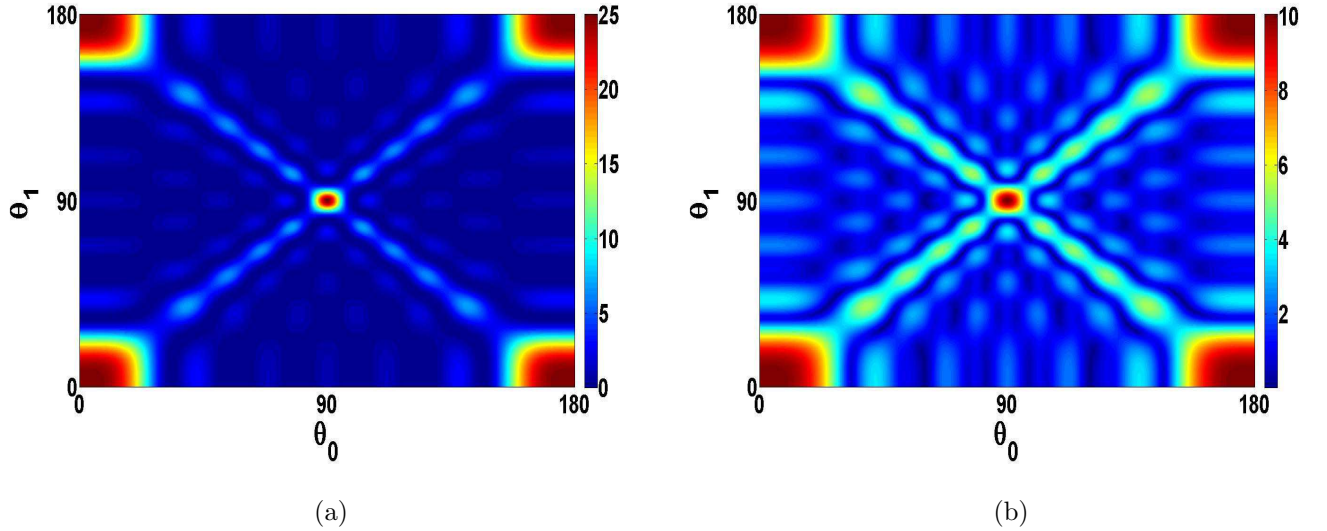


FIG. 4: (Color Online)(a) shows the variation of $|F(\theta_0, \theta_1, K)|^2$ (color axis) with the angles θ_0 and θ_1 . (b) shows the mode splitting $2\mathcal{F}$ Eq.(24) variation (color axis) in units of δ_1 with angles θ_0 and θ_1 , $N=5$, $K=5$, $M=5$. In both cases, θ_0 and θ_1 varies from 0° to 180° .

The photon number and the mode splitting, are given by the expressions (22) and (24) respectively. Both are dependent on the value $|F(\theta_0, \theta_1, K)|^2$ and are thus related to each other. Fig. 4 (a) shows the plot of the $|F(\theta_0, \theta_1, K)|^2$ for $n = 1$ MI state and Fig. 4 (b) shows the mode splitting at specific values of θ_0 and θ_1 and thus very clearly demonstrates their inter-dependence.

This relation is also reflected in the plots of resulting transmission at certain demonstrative values of θ_0, θ_1 as plotted in Fig. 5 and as explained below.

First we consider the case when both θ_0 and θ_1 are being varied from 0° to 180° always maintaining the relation $\theta_0 = \theta_1$. The corresponding $F(\theta_0, \theta_1, K)$ function shows a number

of maxima along the line $\theta_0 = \theta_1$ in Fig. 4(a). The photon number here is given by the expressions (20, 22) where it was seen the normal modes will be zero and $2\mathcal{F}$. In Fig. 5(a) we have plotted this variation in photon number along the color axis as a function of θ_1 and Δ_p/δ_0 . Therefore at each θ_1 one gets a maxima at a value $\frac{\Delta_p}{\delta_0} = 0$ and at twice the value for a single mode case (Fig. 2b).

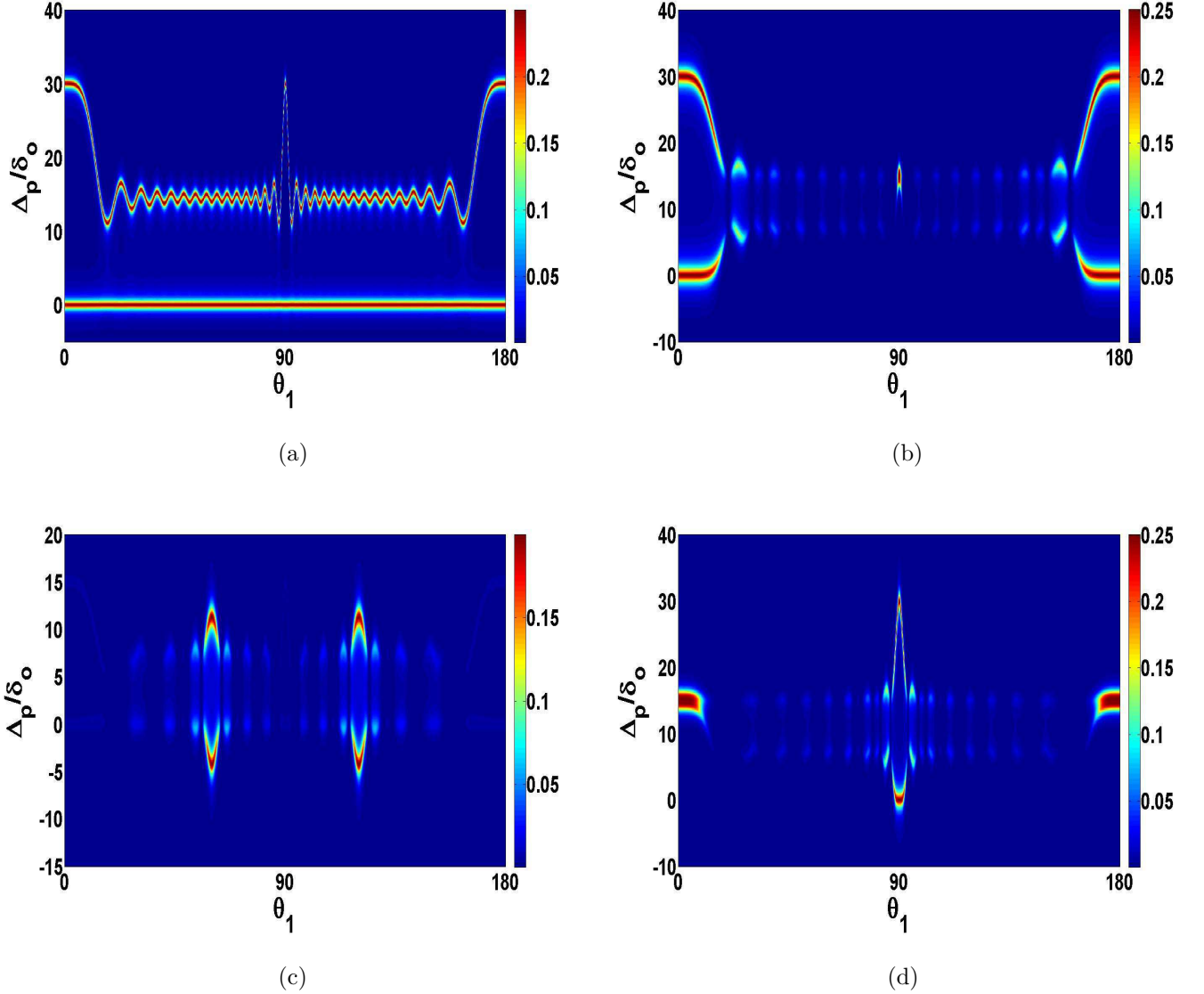


FIG. 5: (Color Online) Variation of the photon number (22) (color axis) with detuning $\frac{\Delta_p}{\delta_0}$ and the angles θ_0 and θ_1 (in degrees) for $N=M=30$, $K=15$, $\kappa=0.5\delta_0$ when the atoms are in MI state, for double standing mode case. In (a) $\theta_0=\theta_1$, $\kappa=0.5\delta_0$. (b) shows the variation when $\theta_0=0^\circ$, θ_1 is varied and $\kappa = \delta$. Similar cases are shown in (c) with $\theta_0=60^\circ$ and in (d) when $\theta_0=90^\circ$

However, in Fig. 5 (b), (c) and (d), we describe the case when θ_0 is kept constant, while the other angle θ_1 is constantly being varied. Corresponding plots show that the maximum number of photons scattered from one mode at an angle θ_0 will be collected by \hat{a}_1 only when $\theta_1 = \pm\theta_0$ or $\pi \pm \theta_0$. When $\theta_1 = \theta_0$, the second mode is parallel to the first mode. When $\theta_1 = -\theta_0$, angle of scattering is equal to the angle of reflection. This is also observed at $\pi \pm \theta_0$ [14]. It is at this co-ordinate, the $|F(\theta_0, \theta_1, K)|^2$, mode splitting as well as the transmitted intensity will show maximum behavior. This is also seen from the $\theta_0 = \theta_1$ and $\theta_0 = \pi - \theta_1$ lines in Fig. 4. For example in (c), when $\theta_0 = 60^\circ$, the plot shows maximum mode splitting and intensity at $\theta_1 = 60^\circ$ and 120° .

One can also study the diffraction pattern of such system in the limit where the shift in the cavity frequency due to dispersion given in (17) is neglected. In that case the transmitted intensity will be directly proportional to the eigenvalue of $\hat{D}_{10}^\dagger \hat{D}_{10}$. This particular limit has been explored in [14, 18, 20] for the two mode case and shown to consist of two parts. The first part is due to classical diffraction and second part shows fluctuations from such classical pattern. The above analysis in this work suggest an enrichment of these diffraction features to a considerable extent once the frequency shift due to diffraction is taken into account.

2. Superfluid

Now we consider that the cold atomic condensate is in SF ground state. The transmission through the SF can be obtained by taking the expectation value of the photon number operator (17) in a SF state. This gives

$$\langle \Psi | \hat{a}_1^\dagger \hat{a}_1 | \Psi \rangle = \frac{1}{M^N} \sum_{\langle n_j \rangle} \frac{N!}{n_1! n_2! \dots n_M!} \frac{\delta_1^2 [F_s(\theta_0, \theta_1, K, n_j)]^2 |\eta_0|^2}{([\Delta_p - (f_{n_j} + \mathcal{F}_{n_j})]^2 + \kappa^2)([\Delta_p - (f_{n_j} - \mathcal{F}_{n_j})]^2 + \kappa^2)} \quad (25)$$

where,

$$f_{n_j} = \frac{\delta_1}{2} (F_s(\theta_1, K, n_j) + F_s(\theta_0, K, n_j))$$

$$\mathcal{F}_{n_j} = \sqrt{\frac{\delta_1^2 (F_s(\theta_1, K, n_j) - F_s(\theta_0, K, n_j))^2}{4} + \delta_1^2 [F_s(\theta_0, \theta_1, K, n_j)]^2}$$

are respectively the eigenvalues of $\hat{\omega}_m$ and $\hat{\Omega}_m$ operators acting on a particular Fock state. These are in terms of $F_s(\theta_0, K, n_j)$ functions which were first described in (14).

$F_s(\theta_0, \theta_1, K, n_j)$ is given by

$$F_s(\theta_0, \theta_1, K, n_j) = \sum_{j=1:K} \cos(j\pi \cos \theta_0) \cos(j\pi \cos \theta_1) n_j \quad (26)$$

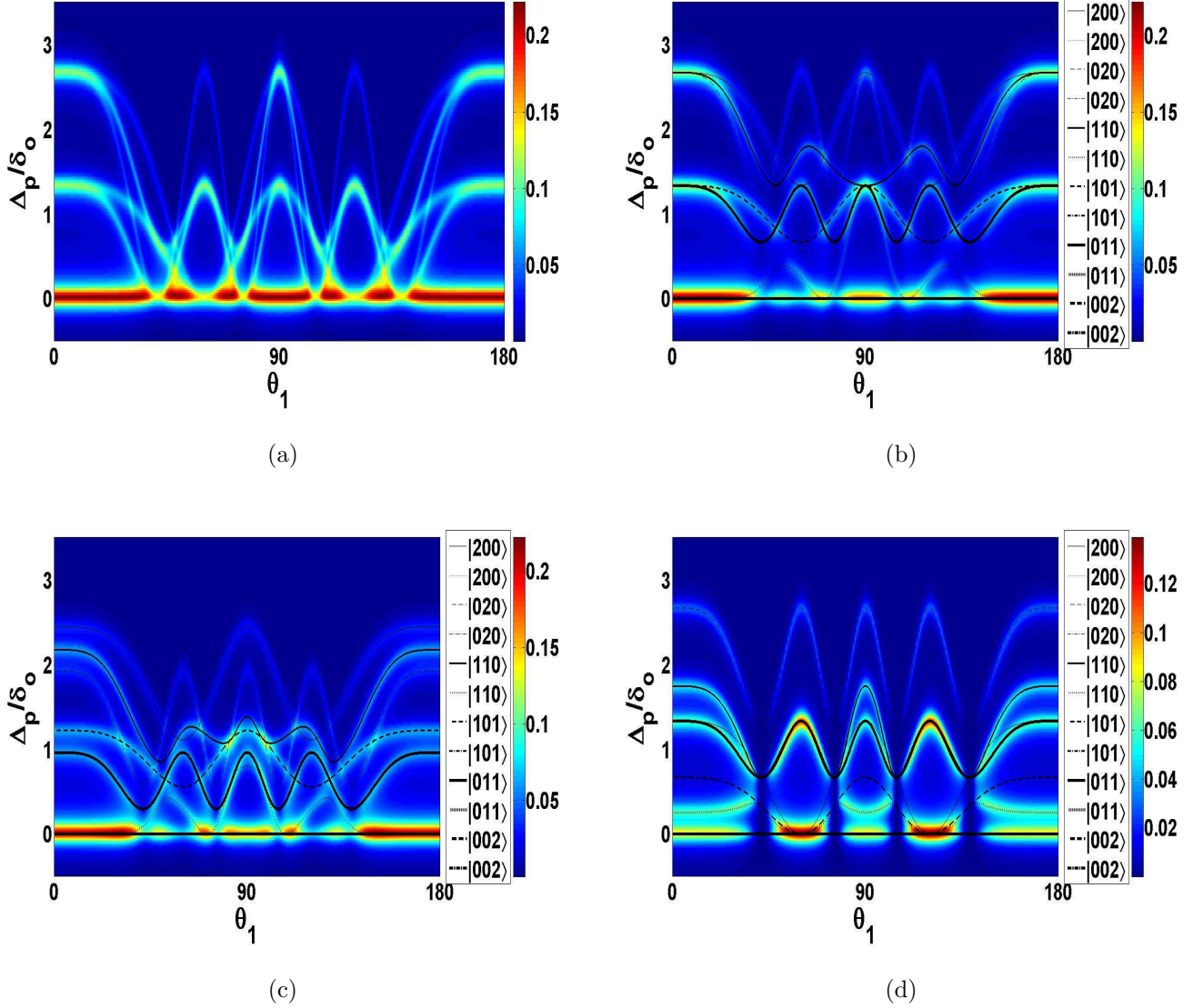


FIG. 6: (Color Online) Variation of the photon number (25) (color axis) with detuning $\frac{\Delta_p}{\delta_o}$ and angles θ_0 and θ_1 (in degrees) for $N=K=2$, $M=3$, $\kappa=0.5\delta_0$ when the atoms are in SF state for double standing mode case, with individual Fock states depicted by black lines; in (a) $\theta_0=\theta_1$ (b) $\theta_0=0^\circ$ (c) $\theta_0=30^\circ$ (d) $\theta_0=60^\circ$

In Fig. 6 (a), the cavity modes are oriented at the same angle with the lattice axis ie. $\theta_0 = \theta_1$, and are together varied from 0° to 180° . Here $F_s(\theta_0, K, n_j) = F_s(\theta_1, K, n_j) =$

$F_s(\theta_0, \theta_1, K, n_j)$ and thus corresponds to the case described in Eq.(20). In this figure, the photon number has been plotted against the angle θ_1 and Δ_p/δ_0 . The plot exhibits that at each angle there is maxima in the photon number when the value of the dispersive shift is either zero or twice its corresponding value for the single mode case.

Fig.6 (b), (c) and (d) describes the variation of the photon number with the angle θ_1 and Δ_p/δ_0 , when one of the modes, θ_0 is kept at a constant angle while the other, θ_1 is changed from 0° to 180° . This makes $F_s(\theta_0, K, n_j)$, $F_s(\theta_1, K, n_j)$ and $F_s(\theta_0, \theta_1, K, n_j)$ change separately for individual Fock states. To understand this, we again consider the case when 2 atoms are placed in 3 sites among which 2 are illuminated. We will have 6 Fock states and the average occupancy will be $2/3$. However each Fock state now gives maximum intensity for two values of Δ_p/δ_o corresponding to the two normal modes $f_{n_j} \pm \mathcal{F}_{n_j}$.

Fig.6(b), shows the intensity distribution when $\theta_0 = 0^\circ$. Here, we observe that when $\theta_1=0^\circ$, the 6 Fock states distribute themselves into groups having 3, 2, 1 states and each group has a distinct value for the dispersion shift depending on the occupancy. However in Fig.6(c) and 6(d), where the angle $\theta_0 = 30^\circ$ and 60° respectively, and the angle θ_1 is varied, we observe the Fock states separate out and each takes a distinct value for the dispersive shift. This allows us to identify each Fock state separately. In Fig.6(d), it is to be noticed that at specific values of θ_1 , the intensity drops to zero, although there is a superposition of the Fock states. This happens as the intensity depending on $F_s(\theta_0, \theta_1, K, n_j)$ becomes zero at these particular values as can be seen from eqs.(25,26).

IV. TRAVELLING WAVES

Fig. 7 depicts our model system where an optical lattice is shown to be illuminated by two ring cavities. We have considered that these cavities allow the waves to propagate only in one direction. Such cavities generate travelling wave modes [36–38]. These modes are described by [8, 36], $u(\mathbf{r}_j)_{TW} = \exp(i(\mathbf{k} \cdot \mathbf{r}_j + \phi))$ where ϕ is constant phase factor which has been set to zero. For such waves, the operator \hat{D}_{00} becomes just

$$\hat{D}_{00} = \sum_{j=1:K} u_l^* u_l \hat{n}_j = \sum_{j=1:K} \hat{n}_j \quad (27)$$

as $u_l^* u_l = 1$. Thus the eigenvalue of \hat{D}_{00} for a given Fock state will be nK which is just the number of atoms in the illuminated sites. Thus the dispersive shift in single mode case will

not depend on the angle θ .

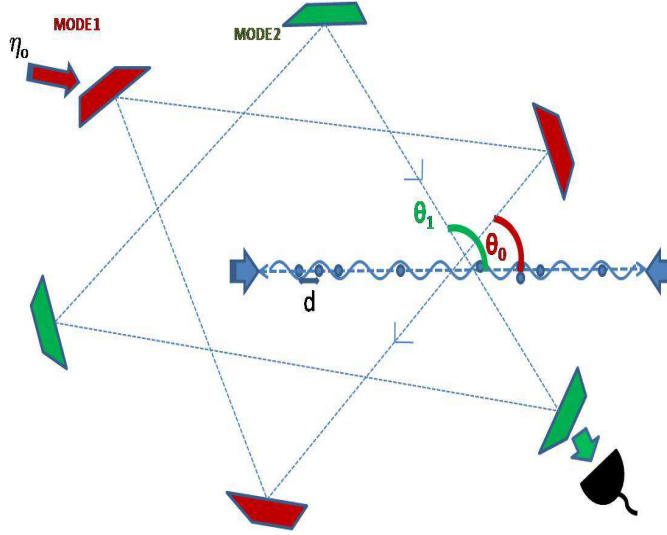


FIG. 7: (Color Online) Schematic diagram of the atom cavity system for travelling wave. The optical lattice is created from two counter propagating laser beams and has a site spacing d . The two ring wave cavity modes, MODE 1 and MODE 2 are at angles θ_0 and θ_1 respectively with the axis of the optical lattice. The MODE 1 is being pumped by a pump laser with amplitude η_0 while MODE 2 is not being pumped but is used to collect the scattered photons by a detector. In the single mode case, the detector is also fixed in MODE 1, and has not been shown in this figure. The ring cavities, are set in a way that the waves is allowed to propagate only in one direction.

However this is not the case when two cavity modes are excited. As we have seen for the case of standing wave, the mode splitting which in turn influences the transmission through such cavity is closely related to the relative angle between the two modes through the function $F(\theta_0, \theta_1, K)$. In the current case the mode splitting is also dependent on the relative angle between the cavity modes since only the eigenvalue of the operator \hat{D}_{10} is angle dependent which is given by,

$$\hat{D}_{10} = \sum_{j=1:K} e^{i(j\pi(\cos\theta_1 - \cos\theta_0))} \hat{n}_j \quad (28)$$

A. Mott Insulator

Again, we first consider the cold atomic condensate in a MI state. The eigenvalue of $\hat{\omega}$ and $\hat{\Omega}$ (16) when acting on the MI state (7) are

$$\begin{aligned} g &= \langle \Psi | \hat{\omega} | \Psi \rangle = \frac{nK\delta_1 + nK\delta_1}{2} = nK\delta_1 \\ \mathcal{G} &= \langle \Psi | \hat{\Omega} | \Psi \rangle = \sqrt{\left(\frac{nK\delta_1 - nK\delta_1}{2}\right)^2 + |G(\theta_0, \theta_1, K)n\delta_1|^2} = |G(\theta_0, \theta_1, K)|n\delta_1 \end{aligned} \quad (29)$$

Here $G(\theta_0, \theta_1, K)$ is

$$G(\theta_0, \theta_1, K) = \frac{\sin(K\pi \frac{\cos\theta_0 - \cos\theta_1}{2})}{\sin(\pi \frac{\cos\theta_0 - \cos\theta_1}{2})} \quad (30)$$

This system is equivalent to two coupled linearized harmonic oscillators (18), but with same natural frequencies ie., $\omega_1 = \omega_2 = \omega_o$ and coupled by a perturbation ζ . The normal modes for such a system is given by $\omega_o \pm \zeta$. In the current problem, the normal modes are hence given by $g \pm \mathcal{G}$ and therefore the amount of mode splitting is $2\mathcal{G}$.

The photon number (17) is,

$$\langle \Psi_{MI} | \hat{a}_1^\dagger \hat{a}_1 | \Psi_{MI} \rangle = \frac{|\eta_0 \mathcal{G}|^2}{([\Delta_p - (g + \mathcal{G})]^2 + \kappa^2)([\Delta_p - (g - \mathcal{G})]^2 + \kappa^2)} \quad (31)$$

Fig. 8 (a) depicts the variation of function $G(\theta_0, \theta_1, K = 5)$ with θ_1 and θ_0 . For a particular value of θ_0 and θ_1 , this function takes the maxima value when the argument of the function, ie., $(\cos\theta_0 - \cos\theta_1)$ will become zero, ie., when $\theta_1 = \pm\theta_0$. This can be seen from the $\theta_0 = \theta_1$ line.

Fig. 8 (b)-(d) depicts the variation of intensity with Δ_p/δ_0 and θ_1 for a fixed value of θ_0 . The plots show two symmetrically placed transmission peaks, whose separation is again proportional to $G(\theta_0, \theta_1, K)$ and therefore will also show a maxima when $\theta_0 = \pm\theta_1$. Physically $\theta_1 = \theta_0$ corresponds to the case when both the ring cavities are oriented at the same angle, while $\theta_0 = -\theta_1$, corresponds to the case when scattering is at the angle of reflection. However, in Fig. 8 (b), when $\theta_0 = 0^\circ$, we observe an additional maxima at $\theta_1 = 180^\circ$ because, at this value, function $G(\theta_0, \theta_1, K) = \frac{\sin(K\pi)}{\sin\pi}$ also shows a maximum behavior (Fig. 8(a)). Also it is clearly seen that in all these plots, both the normal modes symmetrically vary around the average value *i.e.*, nK . This average value is shown by a dotted black line in the Fig. 8 (b). As clearly seen, it is independent of the angles between the lattice axis and the cavity modes, and is only dependent on the total number of atoms present in the illuminated sites.

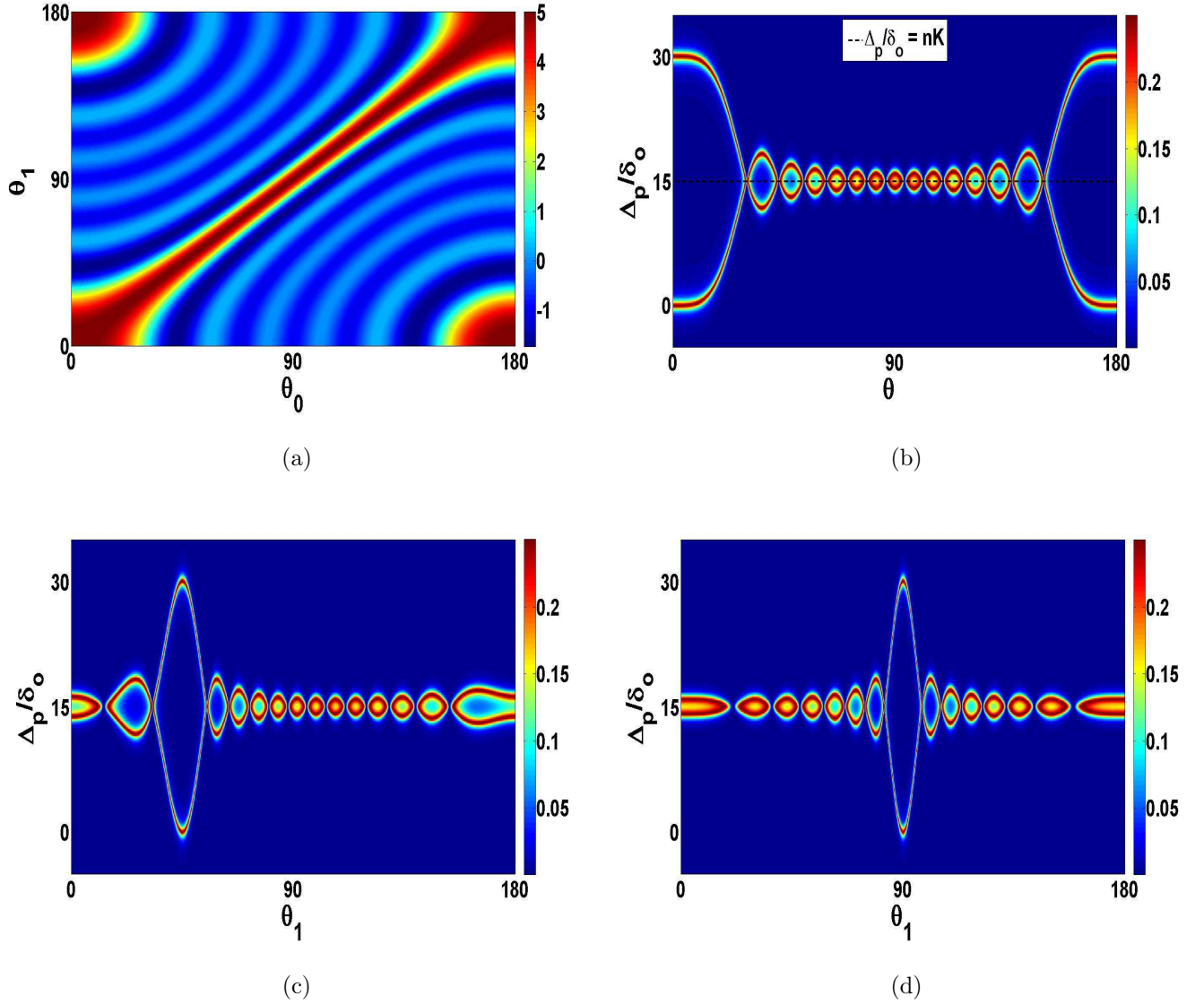


FIG. 8: (Color Online)(a)Variation in $G(\theta_0, \theta_1, K = 5)$ (color axis) with θ_0 and θ_1 (in degrees). (b)Variation of the photon number(color axis) with detuning $\frac{\Delta_p}{\delta}$ and θ_1 (in degrees), $N=M=30$, $K=15$, $\kappa=0.5\delta_0$ when the atoms are in MI state, single travelling mode case. $\theta_0=0^\circ$ (c) $\theta_0= 45^\circ$ (d) $\theta_0= 90^\circ$

B. Superfluid

In this case also, the mode splitting only depends on the eigenvalue of the operator \hat{D}_{10} , but the eigenvalues are different for different Fock states. Fig. 9 depicts the same for travelling mode case.

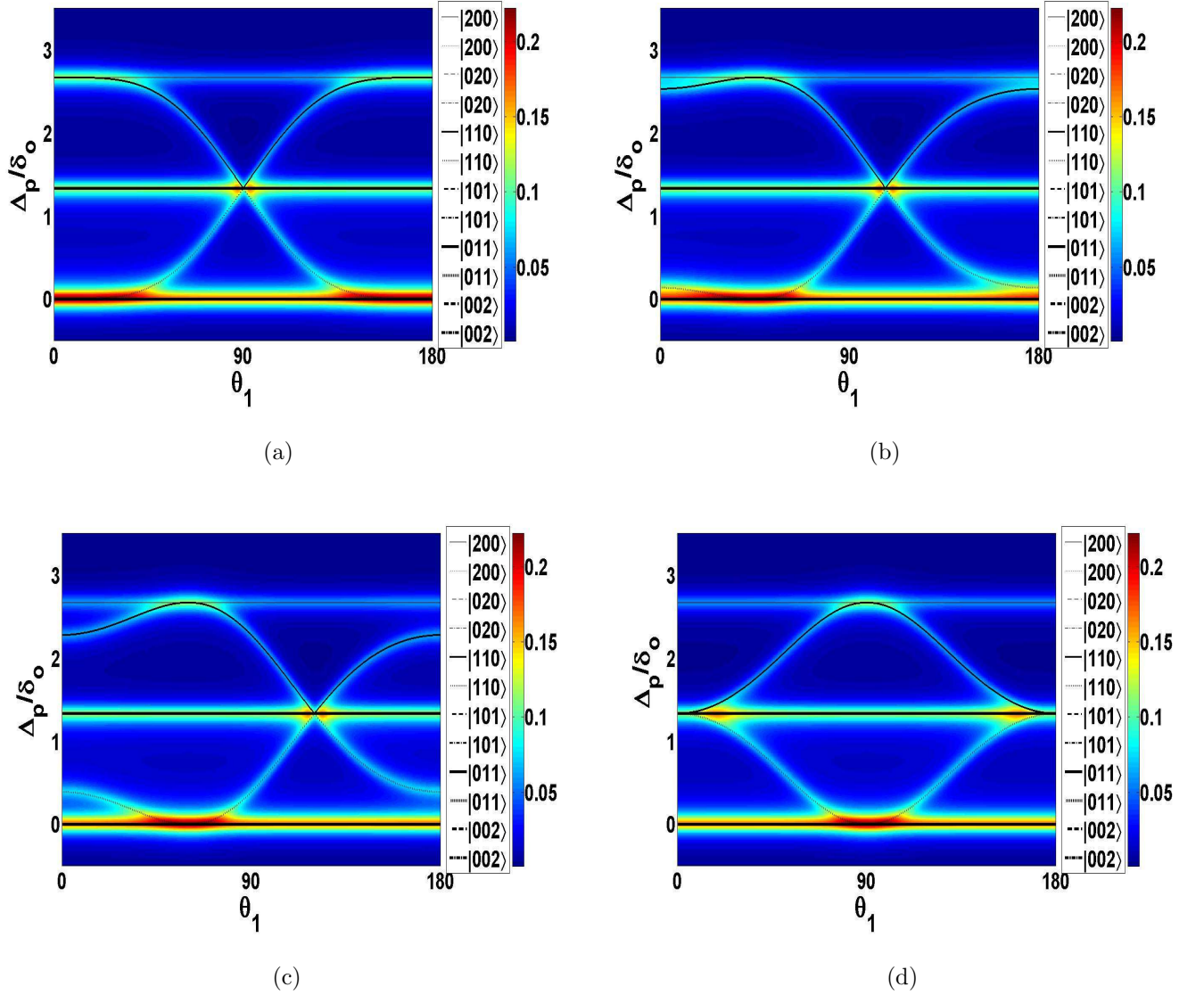


FIG. 9: (Color Online) Variation of the photon number(Color Axis) with detuning $\frac{\Delta_p}{\delta}$ and θ_1 (in degrees), $N=K=2, M=3$, $\kappa=0.1\delta_0$ when the atoms are in SF state, two mode case for travelling wave cavity with individual Fock states depicted by black lines in (a) $\theta_0=0^\circ$ (b) $\theta_0=45^\circ$ (c) $\theta_0=60^\circ$ (d) $\theta_0=90^\circ$

The photon number for this case will be given by,

$$\langle \Psi | a_1^\dagger a_1 | \Psi \rangle = \frac{1}{M^N} \sum_{\langle n_j \rangle} \frac{N!}{n_1! n_2! \dots n_M!} \frac{(\mathcal{G}_s)^2 |\eta_0|^2}{([\Delta_p - (g + \mathcal{G}_s)]^2 + \kappa^2)([\Delta_p - (g - \mathcal{G}_s)]^2 + \kappa^2)} \quad (32)$$

where $g = nK\delta_1$ and $\mathcal{G}_s = G(\theta_0, \theta_1, K, n_j)\delta_1$ where, $G(\theta_0, \theta_1, K, n_j)$ is the eigenvalue of \hat{D}_{10} operator on a Fock state with n_j particles on the j -th site. It may be again noted that in

a SF state n_j varies with the site index j for a given Fock state. The transmission spectra is shown in the Fig.(9) for certain demonstrative values of θ_0, θ_1 . In each case we have also plotted the \mathcal{G}_s for different Fock states which are superposed to form the superfluid.

V. CONCLUSION

In our work, we have analyzed cold atomic condensates formed by bosonic atoms in an optical lattice at ultra cold temperatures. It has been suggested that such system when illuminated by cavity modes, can imprint their characteristics on the transmitted intensity. We have studied the off resonant scattering from such correlated systems by varying the angles that the cavity modes make with the optical lattice and thus obtained the transmission spectrum as a function of the detunings and the dispersive shifts.

The main result of our work reveals the pattern in the shifts of the cavity mode frequency as the relative angle between the cavity mode and the optical lattice is changed. As we have pointed out in section III A 1 that a change in the dispersion shift implies the effective change of the refractive index. Thus our finding implies even for a given quantum phase, as the relative angle between the mode propagation vector and the optical lattice changes, the cavity induced dispersion shift or the effective refractive index of the medium also changes. This highlights the uniqueness of such quantum phase of matter as medium of optical dispersion.

For the single mode case discussed in section III A, in MI phase, we have seen that the transmitted intensity depends on the number of atoms in the illuminated sites, since the presence of an atom shifts the cavity resonance and this shift is directly proportional to the number of illuminated atoms. The SF phase is however a superposition of many Fock states and set of Fock states group correspond to same shift. However changing the angle, these group of Fock states change thus providing more information about the system.

As discussed in next section III B when two cavity modes are considered, the system shows mode splitting between the cavity modes coupled by the atomic ensemble. This was clearly visible in the MI case. In the SF state, at some specific angles of illumination, the Fock states of SF distinctly map to different frequency shift. Thus giving the Fock state structure of the system. However, it was noticed that such a system can only be achieved through high finesse cavities, as such characteristic features in the plots for the SF phase

become blurred for an increase in $\frac{\kappa}{\delta_0}$ values. Such system when illuminated by ring cavities show different features of intensity transmission as shown in the section IV that describes the situation where the cavity modes are travelling waves. Thus the nature of diffraction pattern is also dependent on the nature of the quantization of the electromagnetic wave inside the cavity, which was also mentioned in the earlier work on such quantum diffraction by fermionic cold atoms [31].

As our analysis shows that the variation of the relative angle between the cavity mode and the optical lattice can resolve the Fock space structure of a quantum phase in detail, by varying the effective number of illuminated sites. It has been pointed out in experiment described in ref. [10] that it is possible to study the correlated many body states of few ultra cold atoms in such cavity within the currently available technology. A few body correlated system of ultra cold fermions was also experimentally achieved recently [39]. For example in Fig. 3 and Fig. 6 it has been shown that in the limit of small cavity decay rate κ and for few number of particles in the illuminated site, in a superfluid phase or more correctly a few body analogue of a superfluid state it is possible to identify the extent of superposition in different parameter regime. Such identification is potentially helpful in various type of many body quantum state preparation.

VI. ACKNOWLEDGEMENT

One of us (JL) thanks Prof. H. Ritsch for helpful discussion.

-
- [1] D. Jaksch *et al.*, Phys. Rev. Lett. **81**, 3108 (1998).
 - [2] I. Bloch, J. Dalibard and W. Zwerger, Rev. Mod. Phys. **80**, 885 (2008).
 - [3] M. Greiner *et al.*, Nature **415**, 39 (2002).
 - [4] J. J. Garc a-Ripoll, J. I. Cirac, Phil. Trans. R. Soc. Lond. A **361**, 1537 (2003) .
 - [5] J.M. Raimond, M. Brune, S. Haroche, Rev. Mod. Phys. **73**,565 (2001).
 - [6] O. Morice, Y. Castin and J. Dalibard. Phys. Rev. A **51**, 3896 (1995).
 - [7] M. G. Moore, O. Zobay and P. Meystre, Phys. Rev. A **60**, 1491 (1999).
 - [8] I. B. Mekhov, C. Maschler and H. Ritsch, Nat. Phys **3**, 319 (2007).
 - [9] F. Brennecke *et al.*, Nature **450**, 268 (2007).

- [10] Y. Colombe, T. Steinmetz *et al.*, Nature **450**, 272 (2007).
- [11] F. Brennecke, S. Ritter, T. Donner, T. Esslinger, Science **322**, 235 (2008).
- [12] S. Gupta, K. L. Moore, K. Murch, D. M. Stamper-Kurn, Phys. Rev. Lett **99**, 213601 (2007).
- [13] C. Weitenberg *et al.*, Phys. Rev. Lett. **106**, 215301 (2011).
- [14] I. B. Mekhov, C. Maschler and H. Ritsch, Phys. Rev. A **76**, 053618 (2007).
- [15] I. B. Mekhov, H. Ritsch, Phys. Rev. Lett **102**, 020403 (2009).
- [16] C. Maschler, I.B. Mekhov, H. Ritsch Eur. Phys. J. D **46**, 545 (2008).
- [17] I. B. Mekhov, H. Ritsch, Phys. Rev. A **80**, 013604 (2009).
- [18] I. B. Mekhov, H. Ritsch, Laser Physics, **19**, No. 4, 610 (2009).
- [19] B. Wunsch *et al.*, Phys. Rev. Lett. **107**, 073201 (2011).
- [20] I. B. Mekhov, H. Ritsch, Laser Physics, **20**, No. 3, 694 (2010).
- [21] J. Larson, B. Damski, G. Morigi and M. Lewenstein, Phys. Rev. Lett, **100**, 050401 (2008).
- [22] W. Chen *et al.*, Phys. Rev. A **80**, 011801 (2009).
- [23] W. Chen, D. S. Goldbaum, M. Bhattacharya, P. Meystre, Phys. Rev. A **81**, 053833 (2010)
- [24] A. B. Bhattacharjee, Phys. Rev. A **80**, 043607 (2009); T. Kumar, A. B. Bhattacharjee and ManMohan, Phys. Rev. **81**, 013835 (2010).
- [25] S. Gopalakrishnan, B. L. Lev and P. M. Goldbart, Nat. Phys. **5**, 845 (2009).
- [26] S. Gopalakrishnan, B. L. Lev and P. M. Goldbart, Phys. Rev. A **82**, 043612 (2010)
- [27] S.F. Vidal, G. Chiara, J. Larson, G. Morigi, Phys. Rev. A **81**, 043407 (2010).
- [28] K. Baumann, C. Guerlin, F. Brennecke, T. Esslinger, Nature, **464** 1301 (2010).
- [29] W. E. Frahn, Riv. Nuovo Cim, **7**, 499 (1977).
- [30] H. Tanji-Sujuki *et al.*, Adv. At. Mol. Opt. Phys. **60**, 201 (2011).
- [31] D. Meiser, C. P. Search and P. Meystre, Phys. Rev. A **71**, 013404 (2005).
- [32] M. Born and E. Wolf, Principles of Optics, Cambridge University Press(1999).
- [33] A. Ghatak and K. Thyagarajan, Optical Electronics, Cambridge University Press(1989).
- [34] C. V. Raman and N. S. N. Nath, Proc. Indian Acad. Sci **4**, 222 (1936)
- [35] L. Brillouin, Annales des Physique **17**, 88 (1922).
- [36] M Gangl, H. Ritsch, Phys. Rev. A **61**, 043405 (2000).
- [37] S. Bux *et al.*, Phys. Rev. Lett. **106**, 203601 (2011).
- [38] B. Nagorny, T. Elsässer, A. Hemmerich, Phys. Rev. Lett. **91**, 153003 (2003).
- [39] F. Serwane, G. Zürn, T. Lompe, T. B. Ottenstein, A. N. Wenz and S. Jochim, Science, **332**,

336 (2011).